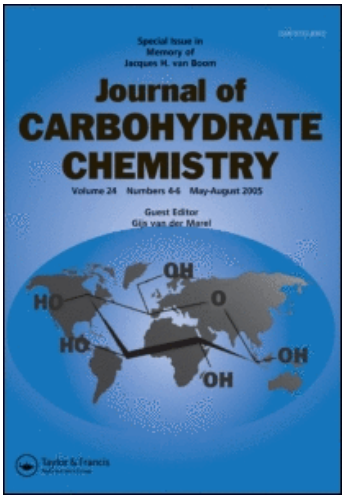

Journal of Carbohydrate Chemistry

Publication details, including instructions for authors and subscription information:
http://www.informaworld.com/smpp/title~content=t713617200

Investigation by NMR Spectroscopy and Molecular Modeling of the Conformations of Some Modified Disaccharide Antigens for *Shigella Dysenteriae* Type 1

Bruce Coxon[a]; Nese Sari[a]; Laurence A. Mulard[b]; Pavol Kovac[b]; Vince Pozsgay[bc]; C. P. J. Glaudemans[b]
[a] Biotechnology Division, National Institute of Standards and Technology, Gaithersburg, Maryland, USA [b] Laboratory of Medicinal Chemistry, National Institute of Diabetes, and Digestive and Kidney Diseases, National Institutes of Health, Bethesda, Maryland, USA [c] Laboratory of Developmental and Molecular Immunity, National Institute of Child Health and Human Development, National Institutes of Health, Bethesda, Maryland, USA

To cite this Article Coxon, Bruce , Sari, Nese , Mulard, Laurence A. , Kovac, Pavol , Pozsgay, Vince and Glaudemans, C. P. J.(1997) 'Investigation by NMR Spectroscopy and Molecular Modeling of the Conformations of Some Modified Disaccharide Antigens for *Shigella Dysenteriae* Type 1', Journal of Carbohydrate Chemistry, 16: 6, 927 — 946
To link to this Article: DOI: 10.1080/07328309708006549
URL: http://dx.doi.org/10.1080/07328309708006549

J. CARBOHYDRATE CHEMISTRY, 16(6), 927-946 (1997)

INVESTIGATION BY NMR SPECTROSCOPY AND MOLECULAR MODELING OF THE CONFORMATIONS OF SOME MODIFIED DISACCHARIDE ANTIGENS FOR *SHIGELLA DYSENTERIAE* TYPE 1

Bruce Coxon,*[a] Nese Sari,[a] Laurence A. Mulard,[b,c] Pavol Kovac,[b]
Vince Pozsgay,[b,d] and C. P. J. Glaudemans [b]

[a]Biotechnology Division, National Institute of Standards and Technology, Gaithersburg, Maryland 20899, USA, [b]Laboratory of Medicinal Chemistry, National Institute of Diabetes, and Digestive and Kidney Diseases, National Institutes of Health, Bethesda, Maryland 20892, USA, [c]Present address: Institut Pasteur, Paris, France, [d]Laboratory of Developmental and Molecular Immunity, National Institute of Child Health and Human Development, National Institutes of Health, Bethesda, Maryland 20892, USA.

Received November 18, 1996 - Final Form March 27, 1997

ABSTRACT

The O-polysaccharide of *Shigella dysenteriae* type 1 is made up of multiple repeats of the linear tetrasaccharide 3)-α-L-Rha*p*-(1→2)-α-D-Gal*p*-(1→3)-α-D-Glc*p*NAc-(1→3)-α-L-Rha*p*-(1→, for which the antigenic determinant for a murine monoclonal IgM antibody is the disaccharide α-L-Rha*p*-(1→2)-α-D-Gal*p*. This disaccharide and various analogs have been studied by 2D NOESY, ROESY, and TOCSY NMR spectroscopy, in conjunction with proton spin-lattice relaxation rate measurements, restrained molecular mechanics, and restrained molecular dynamics with simulated annealing. It has been found that replacement of any single hydroxyl group in the determinant by a hydrogen atom, or replacement of any single hydroxyl group in the Gal residue by a fluorine atom has little if any influence on the conformation of the resulting derivatives.

*Author to whom correspondence should be addressed: Bruce Coxon, A-353 Chemistry, National Institute of Standards and Technology, Gaithersburg, Maryland 20899

INTRODUCTION

The O-specific polysaccharide of *Shigella dysenteriae* type 1 contains the linear tetrasaccharide repeating unit:[1,2]

3)-α-L-Rha*p*-(1→2)-α-D-Gal*p*-(1→3)-α-D-Glc*p*NAc-(1→3)-α-L-Rha*p*-(1→

where Rha*p*, Gal*p*, and Glc*p*NAc stand for rhamnopyranosyl, galactopyranosyl, and 2-acetamido-2-deoxyglucopyranosyl, respectively. Previous studies of a large series of related saccharide methyl glycosides ranging from mono- to octasaccharide derivatives have shown[3] that for a murine monoclonal IgM antibody raised against heat-killed *Shigella dysenteriae* type 1, the principal immunodeterminant is the α-L-Rha*p*-(1→2)-α-D-Gal*p* subunit (hereafter called Rha-Gal). As part of a continuing study of the mechanisms[4] involved in binding of this determinant with the monoclonal antibody under study, a series of deoxy and deoxyfluoro derivatives **2-9** of Rha-Gal-α-OMe (**1**)[5] has been synthesized,[6-8] in which key hydroxyl groups have been specifically replaced by hydrogen or fluorine atoms (**Scheme 1**). Since the conformation of a hapten determinant may play an important role in antibody binding, we wished to define the conformation, and examine whether it is the same for all of its deoxy and deoxyfluoro analogs. Investigations of the related *Shigella flexneri* serogroup antigen by NMR spectroscopy and hard sphere-*exo*-anomeric effect (HSEA) calculations have been reported.[9]

We have used 2D TOCSY NMR methods to confirm the ^{1}H NMR assignments for derivatives **1-9**, and their conformations have been investigated by a combination of measurements of vicinal ^{1}H-^{1}H coupling constants, 2D NOESY and ROESY NMR spectra, ^{1}H spin-lattice relaxation rates by non-, single-, double-, and triple-selective methods, restrained molecular mechanics energy minimization, and restrained molecular dynamics with simulated annealing. Although the 2D NOESY method has been used to survey inter-residue distances in all nine compounds either qualitatively or semi-quantitatively, our concern about the possible influence of spin diffusion on internuclear distances determined by this method led us to verify the distance results for the two key derivatives **1** and **3** by an alternative method, namely the measurement of ^{1}H spin-lattice relaxation rates. Cross-correlation effects[10] can be minimized in relaxation rate measurements by use of the initial slope approximation,[11] in which only the first part of the relaxation curve is analysed and used to

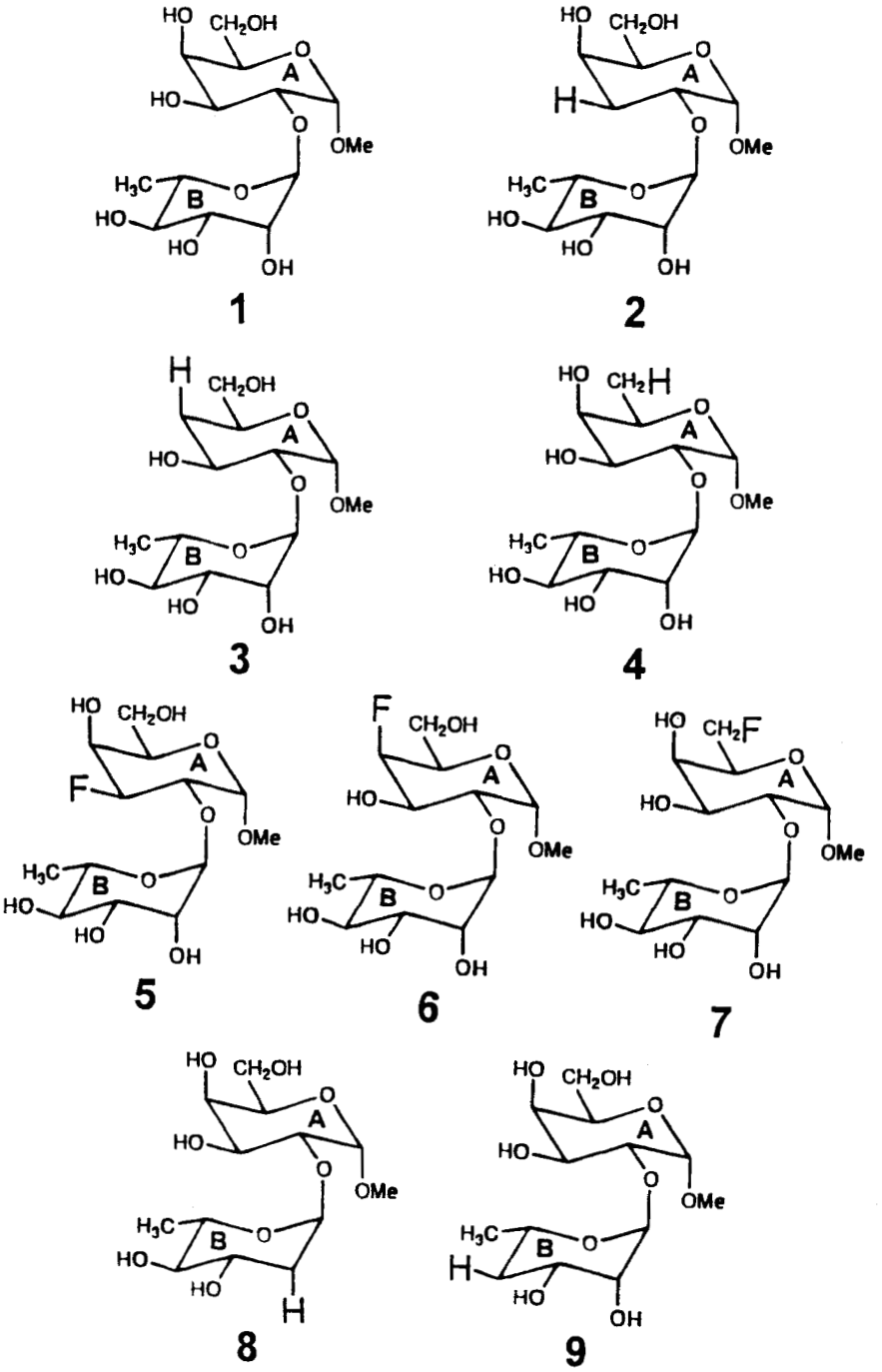

Scheme 1

calculate internuclear distances. The latter procedure is advantageous in that it does not present any particular sensitivity problems. We have also applied the 2D ROESY method to study compound **3**, because in this method, cross peaks that result from spin diffusion have the opposite sign to those that arise from direct dipole-dipole interaction, thus allowing the two phenomena to be distinguished.

RESULTS AND DISCUSSION

NMR spectral assignments and parameters. The ^{1}H NMR spectra of disaccharide derivatives (**1-9**) were mostly well resolved at 500 MHz, and after confirmation of the assignments by interpretation of the TOCSY spectra (as an example, the 2D TOCSY spectrum of the 2-deoxy derivative **8** is shown in **Figure 1**) complete sets of ^{1}H chemical shifts and ^{1}H-^{1}H and ^{1}H-^{19}F spin-spin coupling constants were obtained (see **Tables 1** and **2**, respectively). Some of these values have been reported previously in the synthesis papers,[5-8] based on measurements at 300 MHz. However, the values reported here were measured at 500 MHz under conditions of higher resolution and greater precision. The values of the vicinal ^{1}H-^{1}H coupling constants[12] of the disaccharide derivatives indicate that they exist in the ring forms depicted in the conventional structures (**Scheme 1**, **1-9**).

During the course of this work, we have realized that the ^{13}C-1A and ^{13}C-1B assignments reported earlier[5] for the parent disaccharide **1** should be reversed. The H-1A and H-1B chemical shifts for **1** are very similar (see **Table 1**), but in a 2D ^{13}C-^{1}H chemical shift correlation spectrum of **1** measured at 100.6/400.1 MHz, there is sufficient chemical shift dispersion to allow the upfield H-1A at δ 4.921 to be correlated with the upfield C-1 resonance at δ_C 99.57, which is therefore assigned to C-1A.

TOCSY NMR spectra of Gal residues. A bottleneck is invariably observed in TOCSY experiments for magnetization transfer between H-4 and H-5 of unmodified galactopyranose (Gal) residues,[13-15] if such transfer commences at H-1 (see the 1D slice of the 2D TOCSY spectrum of the specifically monodeoxygenated derivative **8** in **Figure 2a**). This is generally thought to be due to the fact that $J_{4,5}$ is consistently small ($\approx$1 Hz) in Gal residues,[16] which provides an inefficient mechanism for transfer of magnetization from H-4 to H-5 that is mediated by their scalar coupling constant. However, the 2D TOCSY

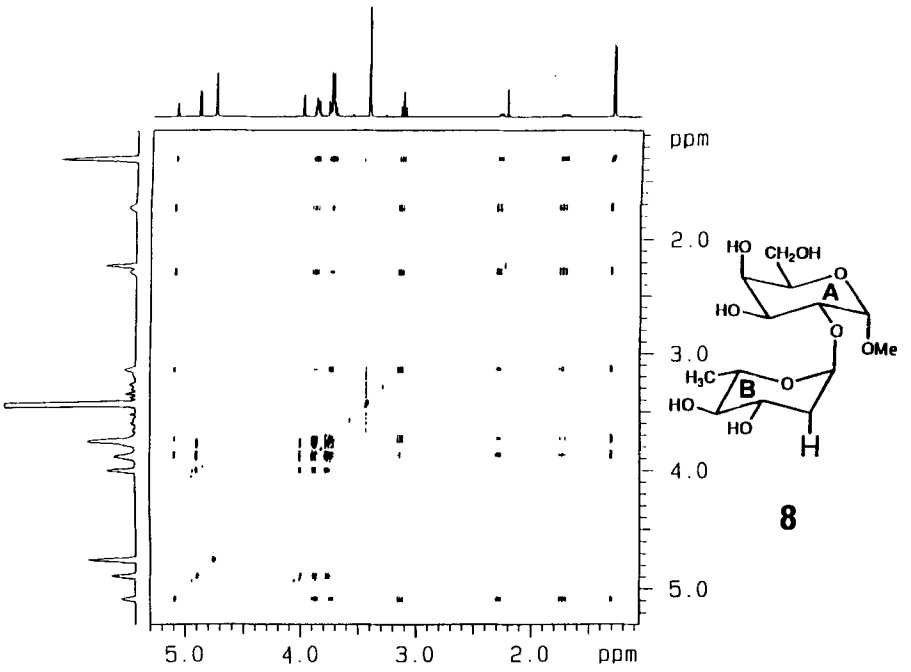

Figure 1. Square contour plot of rectangular 2D TOCSY ^{1}H NMR spectrum of **8** at 500 MHz.

spectrum (see **Figure 3**) of the specifically fluorinated derivative **5** indicates that if this transfer starts at H-4A, then the magnetization transfer bottleneck is not observed, and cross peaks are observed for H-5A, H-6A, and H-6'A, as well as for H-1A, H-2A, and H-3A. Neither is the bottleneck observed in the deoxy derivative **3**, even for H-1A→H-2A→H-3A→H-4A→H-5A transfer, for which there are two reasons. Firstly, there is an additional coupling pathway (H-4aA→H-5A) to H-5A, and secondly, the $J_{4eA,5A}$ coupling is twice as large as in an unmodified galactopyranose residue, due to the lack of an axial electronegative oxygen atom at C-4A of compound **3** (see values in **Table 2**).

TOCSY NMR spectra of Rha residues. In our experience, the generation of 1D TOCSY NMR subspectra of Rha residues by means of the selective excitation of H-1 using a phase gradient frequency offset gives subspectra in which the H-5 signal is weak or undetectable.[13,14] Qualitatively, magnetization that arrives at H-5 appears to transfer rapidly to the H-6 protons, because of the triple coupling pathway to the latter protons. This effect is not seen if the magnetization transfer starts from the H-6 protons of Rha residues, so that

Table 1. ^{1}H NMR chemical shifts[a] of methyl glycosides **1-9**

Proton	Methyl glycoside								
	1	**2**	**3**	**4**	**5**	**6**	**7**	**8**	**9**
1A[b]	4.926	4.872	4.923	4.847	4.983	4.982	4.952	4.890	4.915
2A	3.808	4.038	3.506	3.770	4.131	3.883	3.827	3.765	3.786
3eA[c]	---	2.061	---	---	---	---	---	---	---
3aA	3.881	1.920	3.981	3.885	4.807	3.997	3.905	3.873	3.868
4eA	4.003	4.063	2.010	3.828	4.282	4.916	4.066	3.998	4.000
4aA	---	---	1.491	---	---	---	---	---	---
5A	3.889[d]	3.841	3.913	4.035	3.908	3.975	4.166	3.874	3.884
6A	3.732	3.683	3.592	1.229	3.760	3.791	4.626	3.730	3.730
6'A	3.764	3.718	3.678	1.229	3.797	3.817	4.677	3.760	3.761
OMe	3.433	3.463	3.419	3.412	3.434	3.455	3.439	3.426	3.419
1B	4.934	4.906	4.941	4.927	4.966	4.953	4.941	5.083	4.973
2eB	4.054	3.935	4.060	4.053	4.033	4.051	4.053	2.280	3.880
2aB	---	---	---	---	---	---	---	1.725	---
3B	3.780	3.752	3.781	3.776	3.780	3.780	3.779	3.874	4.048
4eB	---	---	---	---	---	---	---	---	1.768
4aB	3.459	3.444	3.457	3.455	3.463	3.463	3.460	3.131	1.605
5B	3.730	3.722	3.728	3.719	3.722	3.726	3.726	3.733	3.988
6B	1.318	1.311	1.314	1.309	1.320	1.321	1.319	1.306	1.249

a. In ppm, measured at 500 MHz unless stated otherwise, with an estimated standard uncertainty of 0.003 ppm. b. A and B are residue labels, starting at the potential reducing end of the methyl glycoside. c.The labels e and a refer to equatorial and axial hydrogen atoms, respectively. d. Measured at 400 MHz for this proton.

the 1D slice (see **Figure 2b**) taken through the H-6 signal on the diagonal of the 2D TOCSY spectrum (**Figure 1**) of derivative **8** displays an H-5B multiplet of undiminished intensity. In order to obtain good digital resolution in the 1D subspectra produced as slices of 2D TOCSY spectra, the latter spectra were acquired as highly rectangular 2D data matrices (for example, see **Figure 2c** and **EXPERIMENTAL** section).

2D NOESY NMR of Rha-Gal-OMe derivatives. The 2D NOESY NMR spectrum of **3** (see **Figure 4**) is typical in that it shows a large number of *intra*-residue NOEs, but like many oligosaccharides, only a limited number (three, in this case) of conformationally significant, *inter*-residue NOEs.

Table 2. NMR Coupling constants (*J*, Hz) of methyl glycosides **1-9**

Proton	Methyl glycoside								
	1[a]	**2**[b]	**3**[c]	**4**	**5**[d]	**6**[e]	**7**[f]	**8**[g]	**9**[h]
1A,2A	3.8	3.6	3.7	3.9	4.0	3.7	3.8	3.8	3.8
2A,3A	10.3	12.5	9.7	10.3	10.0	10.3	10.3	10.3	10.3
3A,4A	3.3	3.0	5.3	3.4	3.5	2.7	3.4	3.4	3.4
4A,5A	1.1	1.4	2.2	1.2	1.0	<0.4	1.2	1.3	1.1
5A,6A	5.0	7.8	6.4	6.6	4.8	7.2	7.4	5.0	5.0
5A,6'A	7.3	4.3	3.2	6.6	7.5	5.4	3.8	7.2	7.2
6A,6'A	11.7	11.6	12.1	---	11.8	11.8	10.2	11.7	11.7
1B,2B	1.8	1.8	1.8	1.8	1.8	1.8	1.8	1.2	1.9
2B,3B	3.5	3.4	3.4	3.4	3.4	3.5	3.4	5.2	3.2
3B,4B	9.8	9.8	9.8	9.7	8.5	9.8	9.8	9.0	12.1
4B,5B	9.8	9.7	9.6	9.6	9.6	9.6	9.5	9.7	11.6
5B,6B	6.4	6.2	6.3	6.3	6.5	6.3	6.3	6.3	6.3

a. 2B,5B 0.3
b. 1A,3eA 1.0; 2A,3eA 5.1; 3eA,3aA 13.5; 3eA,4A 3.4
c. 3A,4aA 11.5; 4eA,4aA 12.8; 4aA,5A 12.1
d. 1A,F 1.8; 2A,F 11.6; 3A,F 49.0; 4A,F 7.5
e. 2A,F 1.1; 3A,F 29.4; 4A,F 50.6; 5A,F 30.8
f. 5A,F 16.5; 6A,F 48.2; 6'A,F 45.4
g. 1B,2aB 4.0; 2eB,2aB 13.4; 2aB,3B 11.9
h. 3B,4eB 4.8; 4eB,4aB 12.7; 4eB,5B 2.4 Hz.

All nine disaccharide derivatives **1-9** show the same general pattern of *inter*-residue NOEs for proton pairs 1A,5B, 1A,6B, 2A,1B, and 3A,1B (see **Table 3**), indicating that these derivatives have similar conformations.

Spin-lattice relaxation rates. We have measured the non-selective and multi-selective proton relaxation rates of **1** and **3** by using the initial slope approach,[11] and from these rates have calculated interproton distances as described previously.[10,17-20] The non-selective relaxation rate $R_1^I(ns)$ is given[10] by

$$R_1^I(ns) = \sum_{j \neq i} (\rho_{ij} + \sigma_{ij}) + \rho_i^* \qquad (1)$$

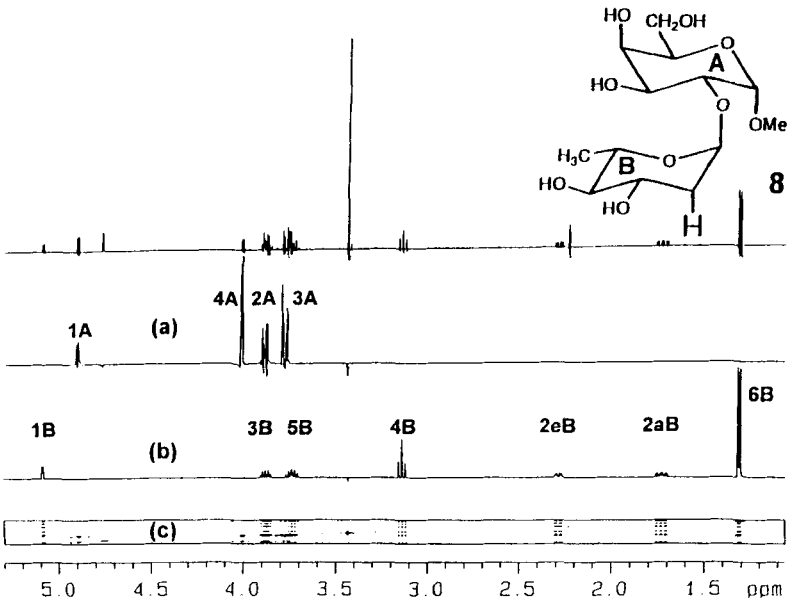

Figure 2. ^{1}H NMR spectra of **8** at 500 MHz. Top trace: 1D spectrum, (a) and (b) 1D slices of 2D TOCSY spectrum, representing residues A and B, repectively, (c) contour plot of rectangular 2D TOCSY spectrum drawn to scale.

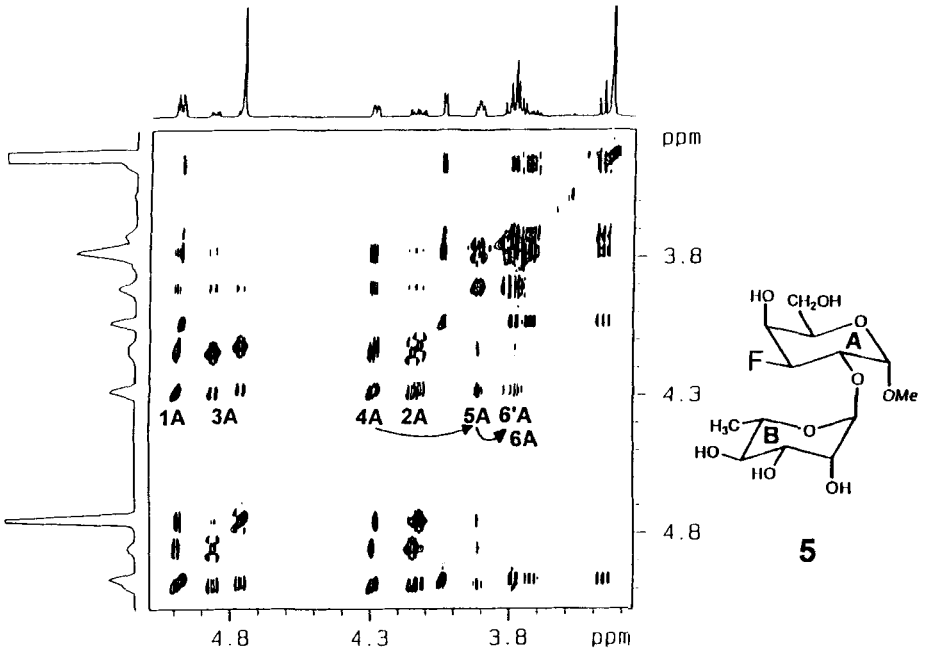

Figure 3. Partial 2D TOCSY ^{1}H NMR spectrum of **5** at 500 MHz, showing H-4A→H-5A→H-6A & H-6' magnetization transfer, i.e., no bottleneck between H-4 and H-5.

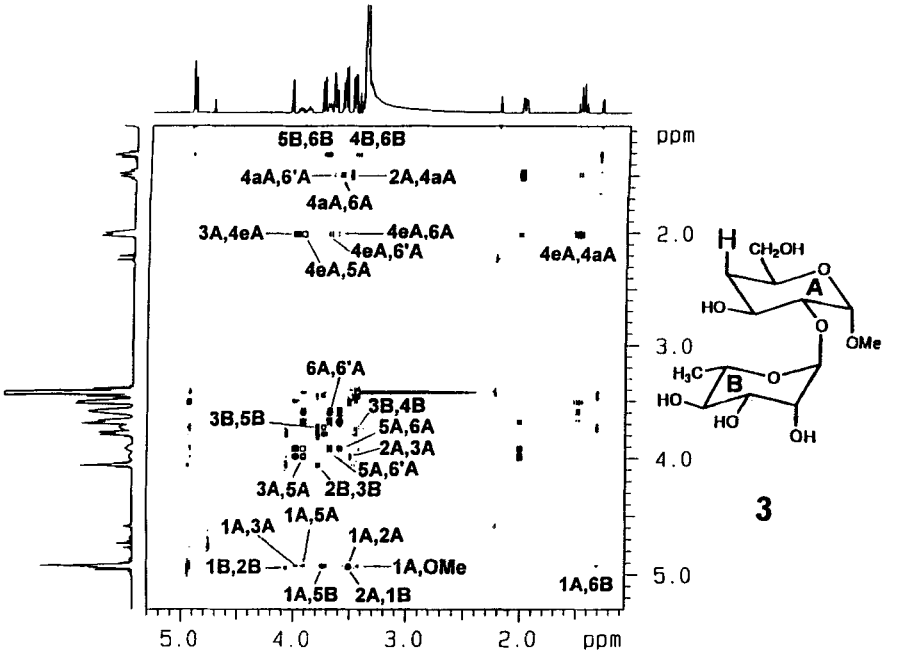

Figure 4. 2D NOESY ^{1}H NMR spectrum of **3** at 500 MHz.

Table 3. Inter-residue NOESY cross peaks of methyl glycosides **1-9**

Proton-proton cross peak	Methyl glycoside								
	1	**2**	**3**	**4**	**5**	**6**	**7**	**8**	**9**
1A,5B	+	+[a]	+	+	+	+	+	+[a]	+
1A,6B	+	+	+	+	+	+	+	+	+
2A,1B	+	+	+	+	+	+	+	+[a]	+
3A,1B	+	+[b]	+[c]	+			+	+[a]	

a. Alternative assignment possible. b. 3eA,1B c. ROESY cross peak.

where ρ_{ij} is the direct, dipole-dipole relaxation between spins *i* and *j* that occurs via single quantum transitions, σ_{ij} is the cross relaxation between spins *i* and *j* which occurs via zero and double quantum transitions, and ρ_i^* is the direct relaxation of spin *i* due to other relaxation mechanisms.

For a single-selective experiment, the spin-lattice relaxation rate is defined[10] by equation *(2)*, where ***i*** indicates that only spin *i* is inverted by a selective 180° pulse.

$$R_1^i(\boldsymbol{i}) = \sum_{j \neq i} \rho_{ij} + \rho_i^* \qquad (2)$$

The double-selective relaxation rates are given by equations *(3)*, where spins *i* and *j* are inverted simultaneously,

$$R_1^{ij}(\boldsymbol{i},\boldsymbol{j}) = \sum_{k \neq i} \rho_{ik} + \sigma_{ij} + \rho_i^*$$
$$R_1^{ij}(\boldsymbol{i},\boldsymbol{j}) = \sum_{k \neq j} \rho_{jk} + \sigma_{ij} + \rho_i^* \qquad (3)$$

and the triple selective rates are described[10] by equations *(4)*,

$$R_1^{ijk}(\boldsymbol{i},\boldsymbol{j},\boldsymbol{k}) = \sum_{n \neq i} \rho_{im} + \sigma_{ij} + \sigma_{ik} + \rho_i^*$$
$$R_1^{ijk}(\boldsymbol{i},\boldsymbol{j},\boldsymbol{k}) = \sum_{n \neq j} \rho_{jn} + \sigma_{ji} + \sigma_{jk} + \rho_i^* \qquad (4)$$
$$R_1^{ijk}(\boldsymbol{i},\boldsymbol{j},\boldsymbol{k}) = \sum_{n \neq k} \rho_{kn} + \sigma_{ki} + \sigma_{kj} + \rho_i^*$$

where spins *i*, *j*, and *k* are inverted at the same time.

The non-, single-, double-, and triple-selective relaxation rates measured for **1** and **3** are shown in **Table 4**. If relaxation is governed solely by ^{1}H-^{1}H dipolar interactions, then the ratio of non-selective to single-selective relaxation rates is[10] $R_1^i(ns)/R_1^i(\boldsymbol{i}) = 1 +$ maximum NOE = 1.5. The experimentally observed deviations from this ratio (see **Table 4**) indicate[10] that other relaxation mechanisms are operating for **1** and **3**. For **1**, the $R_1^i(ns)/R_1^i(\boldsymbol{i})$ ratios are 1.4, except for that of H-6B, which is 1.1. Similarly for **3**, this ratio is in the range 1.2-1.3, except for H-6B and OMe, which show ratios of 1.1 and 1.0, respectively. We attribute the reduction of the ratio from 1.5 to 1.2-1.4 to electron-nuclear dipolar relaxation

Table 4. Proton spin-lattice relaxation rates[a] (s^{-1}) of **1** and **3** in D_2O at 400 MHz and 300 K

Experiment	Proton							
	1A	2A	1B	5B	6B	OMe	3A	5A
non-selective	1.04 (1.05)[b]	1.42 (1.38)	1.04 (1.05)	1.13	1.86 (1.89)	1.095	0.80	1.23
single-selective	0.80 (0.75)	1.09 (0.99)	0.82 (0.75)	0.88	1.64 (1.73)	1.10	0.68	0.94
non-/single-selective	1.23 (1.40)	1.31 (1.40)	1.26 (1.40)	1.28	1.13 (1.09)	1.00	1.18	1.31
double-selective								
R_1 (1A,5B)	0.85			0.98				
R_1 (1A,6B)	0.825 (0.83)				1.83 (1.74)			
R_1 (1A,OMe)	0.92					1.21		
R_1 (3A,5A)							0.765	1.02
triple-selective								
R_1 (1A,1B,2A)	0.96 (0.905)	1.43 (1.20)	1.05 (0.98)					
R_1 (1A,1B,3A)	0.81		0.87				0.71	

a. Estimated standard uncertainty derived from least squares fit 2 %. b. The values for **1** are shown in parentheses.

contributions from paramagnetic oxygen in the solutions, which were not degassed. For H-6B and OMe, the further reductions in the ratio from 1.2-1.4 to 1.0-1.1 are attributable to the spin rotation mechanism, which is known to be significant for methyl protons. The problem of incomplete, intramolecular ^1H-^1H dipolar relaxation was circumvented by the use of subtractive combinations of the single-, double-, and triple-selective rate equations (*2*, *3*, and *4*), which caused the rate of relaxation ρ_i^* by other mechanisms to cancel out.

In the extreme narrowing limit for a rigid molecule tumbling isotropically in solution, the internuclear distance r_{ij} between spins *i* and *j* is described[10] by equation *(5)*,

$$-2\sigma_{ij} = \rho_{ij} = \frac{\gamma_i^2\gamma_j^2\hbar^2}{r_{ij}^6}.\tau_c \qquad (5)$$

where γ_i and γ_j are the gyromagnetic ratios of spins *i* and *j*, $\hbar$ is Planck's constant divided by 2π, and τ_c is the rotational correlation time during which the molecule reorients through an angle of one radian. From measurements of the ^{13}C spin-lattice relaxation times of **3** we determined the value τ_c 8.21 x 10^{-11} s, which, together with the cross relaxation terms σ_{ij} calculated from equations *(2-4)* allowed determination of values of r_{ij} by use of equation *(5)*.

Distance information was also derived from σ_{ij} terms that were determined by combining non-selective relaxation rates with either double- or triple-selective relaxation rates, in equations *(6)* and *(7)*, respectively

$$\sigma_{ij} = 3R_1^i(i,j) - 2R_1^i(ns) \qquad (6)$$

Values for the distances calculated from the relaxation rates of **1** and **3** are shown in **Table 5**. In view of the approximations that are inherent in both the relaxation rate and NOESY approaches, the distances obtained by combining the double- and single- selective

$$\begin{bmatrix} 1 & 1 & 0 \\ 1 & 0 & 1 \\ 0 & 1 & 1 \end{bmatrix} \begin{bmatrix} \sigma_{ij} \\ \sigma_{ik} \\ \sigma_{jk} \end{bmatrix} = \frac{1}{3} \begin{bmatrix} R_1^i \\ R_1^j \\ R_1^k \end{bmatrix} \qquad (7)$$

where $R_1^i = 3R_1^i(i,j,k) - 2R_1^i(ns)$

Table 5. Interproton distances[a] (Å) for **1** and **3**.

Experiment	Proton pair							
	1A,2A	1B,2A	1A,5B	1A,6B	1A,OMe	1A,3A	1B,3A	3A,5A
double- and single-selective			2.6	3.1	2.6			2.6
double- and non-selective			2.2	2.1	2.0			2.2
triple- and double-selective	2.4 (2.3)[b]	2.2 (2.2)		(3.4, 2.6)		3.5	3.6	
triple- and non-selective	2.1	2.1				2.7	2.4	
2D NOESY-RMM[c]	2.4	2.2	2.3	2.8	2.4	3.8	4.3	2.6
				3.9	2.9			
				4.2	3.55			

a. Estimated standard uncertainty 0.1 Å. b. The interproton distances for **1** are shown in parentheses. c. Restrained molecular mechanics

rates, or the triple- and double-selective rates are in reasonable agreement with the results derived from the NOESY data. However, the results from combinations of double- and non-selective data, or triple- and non-selective data deviate from the NOESY derived values to a greater extent. This appears to be because the contributions from the other relaxation mechanisms are not canceled out when the triple- or double-selective rates are subtracted from the non-selective rates.

Our initial slope approximation extends over an inversion recovery variable delay range of one second, which corresponds to the range of mixing times that were used to calculate distances in the NOESY method. Since no deviations from exponential behavior have been observed in this initial slope approximation (in the form of oscillatory excursions from a linear, semilogarithmic plot of magnetization versus delay time[10]), we conclude that spin diffusion is not a problem in these disaccharide NOESY experiments, when they are conducted with mixing times in a range of up to at least one second. Some tricyclic monosaccharide or disaccharide derivatives have not shown any deviations from exponential behavior over time frames as large as 1.5 to 5 seconds.[10]

2D ROESY NMR of 3. Measured at 500 MHz and with the diagonal peaks phased negative, the 2D ROESY spectrum of **3** showed positive cross peaks for the inter-residue proton pairs 1A,3B, 1A,5B, 2A,1B, and 3A,1B, and also for several intra-residue pairs such as 1A,2A, 1A,3A, 1A,5A, and 1A,OMe. No cross peak was detected for 1A,6B in the ROESY spectrum, apparently because of the canceling effect of strong, negative t_1 noise that was not readily removed from this spectrum by mean row subtraction. The 3A,1B cross peak was not observed in the 2D NOESY spectrum of **3**, but did appear in the NOESY spectra of derivatives **1**, **2**, **4**, **7**, and **8** (see **Table 3**). A number of cross peaks in the midfield region of the 2D ROESY spectrum of **3** displayed both positive and negative components, which we interpret as mixtures of intra-residue, ROESY dipolar and TOCSY correlation cross peaks, for example, 2B,3B, 5A,6A, and 5A,6'A. Since the inter-residue cross peaks 1A,3B, 1A,5B, 2A,1B, and 3A,1B have opposite phase to the diagonal peaks and the TOCSY cross peaks, and also show no negative components, we can conclude that these inter-residue cross peaks do not arise by spin diffusion.

Molecular mechanics and dynamics. The apparent proximity (≤4 Å) of the protons in the pairs 1A,5B, 1A,6B, 2A,1B, and 3A,1B was used to generate a starting conformation

for molecular mechanics computations,[21-25] by rotation of the sugar residues in compound **1** about their interglycosidic bonds. Energy minimization of this starting structure using an unmodified AMBER forcefield then yielded a value (2.5 Å) for the H-3A-H-5A distance in the Gal residue of **1** that was used as a reference distance in the AURELIA program to compute inter-residue, internuclear distances from the NOE intensities measured by this program. For example, AURELIA analysis of the intensities of the three inter-residue NOEs for derivative **3** yielded 1A,5B, 1A,6B, and 2A,1B distances of 2.1, 2.9, and 2.0 Å, respectively. The application of these distances as restraints in molecular mechanics (RMM) computations (*in vacuo*) yielded the energy minimized conformation shown in **Figure 5**, in which the 1A,5B, 1A,6B, and 2A,1B distances are 2.3, 2.8, and 2.2 Å, respectively. A conformation similar to that shown in **Figure 5** was obtained by the application of restrained molecular dynamics with simulated annealing (RMD-SA), together with the AURELIA generated restraints, at a dielectric constant of 77.9 (D_2O). In these computations, the use of the AMBER forcefield with Homans extensions yielded a conformation in which the 1A,5B, 1A,6B, and 2A,1B distances were 2.2, 2.9, and 2.3 Å, respectively, whereas the use of the CFF91 forcefield yielded similar distances of 2.3, 2.9, and 2.2 Å, respectively. In the conformation depicted in **Figure 5**, H-1A is close to H-3B. The observation of a positive 1A,3B cross peak in the 2D ROESY NMR spectrum of **3** is consistent with this proximity.

The interglycosidic angles ϕ = -69.5° (O-5B-C-1B-O-1B-C-2A) and ψ = 98.6° (C-1B-O-1B-C-2A-C-1A) that were determined by RMM of derivative **3** are in good agreement with the values (-69.6° and 101.6°, respectively) that were obtained from GESA computations in which a full search of ϕ/ψ conformational space was made.[26] RMD-SA of **3** with the modified AMBER forcefield generated a conformation having ϕ = -65.1° and ψ = 109.4°, whereas the use of the CFF91 forcefield produced dihedral angles ϕ = -70.1° and ψ = 107.8°. All of these methods have yielded results that appear to be consistent with a single conformation, in contrast to earlier results for 2,3,4,6,2',3'-hexa-*O*-acetyl-4-*O*-α-D-glucopyranosyl-1',6'-anhydro-β-D-glucopyranose, for which computer simulation has indicated several sets of ϕ and ψ angles that are consistent with the NMR-determined parameters.[27] However, the calculation of either single or multiple conformations by empirical molecular mechanics methods may be somewhat method dependent. The validity of our analysis of the NOESY data for **3** was confirmed by back-calculation of a theoretical

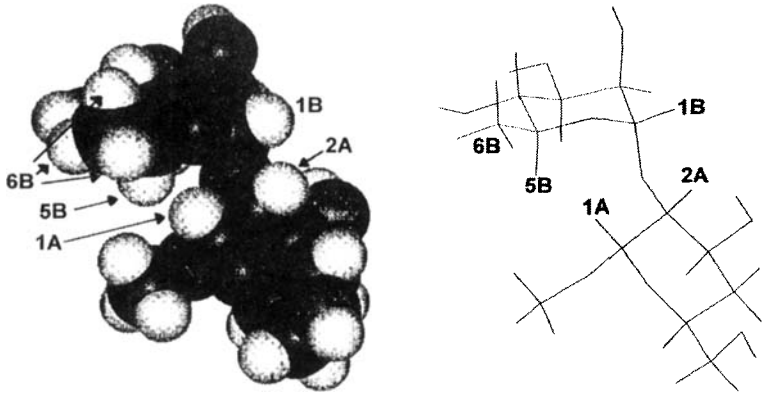

Figure 5. Conformation of **3** from a molecular mechanics computation restrained to distances calculated from the inter-residue NOEs.

2D NOESY spectrum from the structure shown in **Figure 5**. The resulting spectrum agreed well with the experimental 2D NOESY spectrum.

CONCLUSIONS

NMR and molecular mechanics and dynamics studies of α-L-Rha*p*-(1→2)-α-D-Gal*p*-OMe (**1**) and eight of its deoxy and deoxyfluoro derivatives (**2-9**) have shown that these derivatives all adopt the same conformation (see **Figure 5**) in which all of the hydroxyl groups except that at C-4 of the rhamnose residue lie on one side of the molecule. This steric arrangement would be expected to permit significant hydrogen bonding interactions[28] of the disaccharide with an antibody pocket, without changing the carbohydrate conformation.

EXPERIMENTAL

NMR Spectroscopy. ^{1}H NMR spectra were measured at 300 K at either 400 or 500 MHz, by use of Bruker Instruments* WM-400 or AMX-500 spectrometers, respectively.

*Certain commercial equipment, instruments, or materials are identified in this paper to specify adequately the experimental procedure. Such identification does not imply recommendation by the National Institute of Standards and Technology, nor does it imply that the materials are necessarily the best available for the purpose.

Solutions of each disaccharide methyl glycoside (20 mg) in deuterium oxide (0.5 mL) were used without deoxygenation, with a trace of acetone added as a secondary internal reference and assigned as δ 2.225. 1D NMR spectra were acquired at 500 MHz by using a π/2 pulse (9.8 μs) with a 2.4 kHz spectral width, a 3.8 s pulse recycle time, a 16384 point data set zero-filled to 32768 points, and resolution enhancement by Gaussian multiplication, using a Gaussian broadening fraction of 0.3, with a line broadening of -1.0 to -3.5 Hz. Because the 500 MHz spectrometer used for this work had only old software installed (UXNMR[29] vs. 901001.6), selective 1D TOCSY[30,31] spectra excited by phase gradient frequency offset irradiation of anomeric protons were not available. Therefore, useful 1D TOCSY subspectra of individual sugar residues were obtained as F_2 slices of highly rectangular 2D TOCSY spectra. The latter spectra were acquired by using 8192 (F_2) x 256 (F_1) data sets, zero-filled to 16384 x 512 points, together with spectral widths of 2.4 kHz in both dimensions, a mixing time of 200 ms, and an experiment time of 75 min. A sine bell window function shifted by π/4 rad was applied to both dimensions. These conditions afforded digital resolution of 0.144 Hz/point (F_2) and 4.61 Hz/point (F_1), thus giving good resolution in F_2 slices.

2D NOESY[32] NMR spectra were recorded by use of 2048 (F_2) x 512 (F_1) point data sets, zero-filled to 2048 points in the F_1 dimension, together with mixing times of 0.25, 0.5, 1, or 2 s, a sine bell window function shifted by π/2 rad and applied to both dimensions, and a digital resolution of 1.15 Hz in each dimension. 2D ROESY[33,34] NMR spectra were obtained under similar conditions, except that a spectral width of 2.0 kHz was used in both dimensions, together with a spin-lock mixing time of 125 ms. All 2D NMR spectra were acquired with simultaneous quadrature sampling in States-TPPI mode.

^{1}H T_1 values were measured by the inversion recovery method[35] at 400 MHz by using the ^{1}H decoupler unit of the Bruker WM-400 spectrometer to generate all excitation pulses in the non-, single-, and double-selective modes. A train of two sequential frequency switched, selective inversion pulses was used for the double-selective mode, which also served as a triple-selective mode in cases where two of the three nuclei to be selectively excited had very similar chemical shifts (for example H-1A and H1-B). The data were acquired by use of the Bruker DISR94 program,[29] version 940401.0, running on the Aspect 3000 data system. The π/2 pulse width for hard pulses was 12.9 μs, whereas the π pulse

width for selective, soft inversion pulses was 25 ms. A spectral width of 2.5 kHz was used, together with 32768 point data sets, 52 delay times in the range 0.01-8 s, 8 or 16 scans per spectrum, and 2 or 4 cycles through each set of delay times.

Data Processing and Analysis. Most 1D and 2D NMR data were processed and analysed by use of either Silicon Graphics Inc. Indigo R-3000 (33 MHz) or Indigo^2 R-4400 (200 MHz) workstations, using either the Bruker UXNMR version 941001.1 and AURELIA version 941101.1 programs,[29] or XWINNMR version 1.2 and AURELIA version 2.0 programs,[29] respectively. Interpretation of the NOE intensities was based on the isolated spin pair approximation and on the assumption of a single, predominant conformational state for each disaccharide derivative. NOE back-calculation was performed in the complete relaxation matrix analysis module of AURELIA. Inversion recovery data were processed in the relaxation time module of the DISR94 program[29] version 940401.0, using a three parameter, exponential fit for calculation of the T_1 values. Data for the initial slope approximation were obtained from the first 36 spectra out of the total of 52 spectra, corresponding to a delay time range of 0.01-1 s.

Molecular Modeling. The initial molecular modeling of the disaccharide structures was performed with the HYPERCHEM version 4.0 and CHEMPLUS version 1.0A programs[36] running on an Accel PC 486 DX2/66. An unmodified AMBER forcefield was used for these molecular mechanics calculations, together with a distance dependent dielectric, and a Polak-Ribiere conjugate gradient algorithm. Restrained molecular dynamics with energy minimization and simulated annealing were performed with Biosym Insight II version 3.0.0 and Discover version 95.0/3.0.0 software,[37] running on a Silicon Graphics Inc. Indigo^2 R-4400 (200 MHz) workstation. Conformations drawn from Scheme 1 were used as starting structures for restrained molecular dynamics/energy minimization computations, which were conducted at a dielectric constant of 77.9, with a distance dependent dielectric, using either the CFF91 forcefield, or the AMBER forcefield with Homans' modifications.[38] The penalties for violation of the distance restraints were set at 5 and 10 kcal mol^{-1} Å^{-1} for the upper and lower bounds, respectively. In a typical molecular dynamics run with simulated annealing, an initial energy minimization was performed by using a steepest descent algorithm for 500 iterations, the system was then heated to 800 K, and restrained molecular dynamics

was run for 1000, 1 fs steps, followed by 5000 steps at the same temperature, and then 5000 steps at each of a series of temperatures decremented by 50 K each time, down to 300 K. Equilibration was then assessed by performing 10-12 more restrained molecular dynamics simulations for 5 ps each, at 300 K. Energy minimization was performed after every 1 ps or 5 ps dynamics run by use of <200 iterations of the VA09A algorithm.

ACKNOWLEDGMENTS

Thanks are due Dr. John Orban for access to the Bruker AMX-500 NMR spectrometer at the Center for Advanced Research in Biotechnology, and Dr. P. G. Nyholm for discussion.

REFERENCES

1. B. A. Dmitriev, Yu. A. Knirel, N. K. Kochetkov, and I. L. Hofman, *Eur. J. Biochem.*, **66**, 559 (1976).
2. S. Sturm, B. Jann, P. Fortnagel, and K. N. Timmis, *Microb. Pathog.*, **1**, 307 (1986).
3. V. Pavliak, E. M. Nashed, V. Pozsgay, P. Kovac, A. Karpas, C. Chu, R. Schneerson, J. B. Robbins, and C. P. J. Glaudemans, *J. Biol. Chem.*, **268**, 25797 (1993).
4. C. P. J. Glaudemans, *Chem. Rev.*, **91**, 25 (1991).
5. P. Kovac and K. J. Edgar, *J. Org. Chem.*, **57**, 2455 (1992).
6. L. A. Mulard, P. Kovac, and C. P. J. Glaudemans, *Carbohydr. Res.*, **251**, 213 (1994).
7. L. A. Mulard, P. Kovac, and C. P. J. Glaudemans, *Carbohydr. Res.*, **259**, 21 (1994).
8. L. A. Mulard and C. P. J. Glaudemans, *Carbohydr. Res.*, **274**, 209 (1995).
9. K. Bock, S. Josephson, and D. R. Bundle, *J. Chem. Soc., Perkin Trans. 2*, 59 (1982).
10. P. Dais and A. S. Perlin, *Adv. Carbohydr. Chem. Biochem.*, **45**, 125 (1987).
11. R. Freeman, S. Wittekoek, and R. R. Ernst, *J. Chem. Phys.*, 1529 (1970).
12. B. Coxon, *Tetrahedron*, **21**, 3481 (1966).
13 V. Pozsgay, B. Coxon, and H. Yeh, *Bioorg. Med. Chem.* **1**, 237 (1993).
14. V. Pozsgay and B. Coxon, *Carbohydr. Res.*, **257**, 189 (1994).
15. V. Pozsgay and B. Coxon, *Carbohydr. Res.*, **277**, 171 (1995).
16. B. Coxon and H. G. Fletcher, Jr., *Chem. & Ind.*, 662 (1964).
17. L. D. Hall, K. F. Wong, and H. D. W. Hill, *J. Chem. Soc., Chem. Commun.*, 951 (1979).
18. L. D. Hall, K. F. Wong, W. E. Hull, and J. D. Stevens, *J. Chem. Soc., Chem. Commun.*, 953 (1979).
19. L. D. Hall and H. D. W. Hill, *J. Am. Chem. Soc.*, **98**, 1269 (1976).
20. P. Dais, T. K. M. Shing, and A. S. Perlin, *J. Am. Chem. Soc.*, **106**, 3082 (1984).
21. A. D. French and J. W. Brady, in *Computer Modeling of Carbohydrate Molecules*, ACS Symposium Series No. 430, A. D. French and J. W. Brady, Eds., The American Chemical Society, 1 (1990).

22. G. Widmalm, R. A. Byrd, and W. Egan, *Carbohydr. Res.*, **229**, 195 (1992).
23. D. C. Lankin, S. T. Nugent, and S. N. Rao, *Carbohydr. Res.*, **229**, 245 (1992).
24. A. D. French and M. K. Dowd, *J. Mol. Struct. (Theochem)*, **286**, 183 (1993).
25. M. K. Dowd, A. D. French, and P. J. Reilly, *J. Carbohydr. Chem.*, **14**, 589 (1995).
26. L. A. Mulard, P. G. Nyholm, and C. P. J. Glaudemans, unpublished work.
27. P. Dais and A. S. Perlin, *Magn. Reson. Chem.*, **26**, 373 (1988).
28. S. R. Arepalli, C. P. J. Glaudemans, G. D. Daves, Jr., P. Kovac, and A. Bax, *J. Magn. Reson.*, Series B, **106**, 195 (1995).
29. Software products of Bruker Instruments Inc., 19 Fortune Drive, Manning Park, Billerica, MA 01821.
30. L. Braunschweiler and R. R. Ernst, *J. Magn. Reson.*, **53**, 521 (1983).
31. A. Bax and D. G. Davis, *J. Magn. Reson.*, **65**, 355 (1985).
32. J. Jeener, B. H. Meier, P. Bachmann, and R. R. Ernst, *J. Chem. Phys.*, **71**, 4546 (1979).
33. A. A. Bothner-By, R. L. Stephens, J. M. Lee, C. D. Warren, and R. W. Jeanloz, *J. Am. Chem. Soc.*, **106**, 811 (1984).
34. A. Bax and D. G. Davis, *J. Magn. Reson.*, **63**, 207 (1985).
35. R. L. Vold, J. S. Waugh, M. P. Klein, and D. E. Phelps, *J. Chem. Phys.*, **48**, 3831 (1968).
36. Products of Hypercube, Inc., Scientific Software, 419 Phillip Street, Waterloo, ON N2L 3X2, Canada.
37. Software products of Biosym/Molecular Simulations Inc., 9685 Scranton Road, San Diego, CA 92121-3752.
38. S. W. Homans, *Biochemistry*, **29**, 9110 (1990).